Soft Matter

PAPER

View Article Online
View Journal

Cite this: DOI: 10.1039/c5sm01002k

Bacterial lipopolysaccharides form physically cross-linked, two-dimensional gels in the presence of divalent cations†

Moritz Herrmann,[a] Emanuel Schneck,‡[a] Thomas Gutsmann,[b] Klaus Brandenburg[b] and Motomu Tanaka*[ac]

Received 27th April 2015,
Accepted 26th June 2015

DOI: 10.1039/c5sm01002k

www.rsc.org/softmatter

We established a bacterial membrane model with monolayers of bacterial lipopolysaccharides (LPS Re and LPS Ra) and quantified their viscoelastic properties by using an interfacial stress rheometer coupled to a Langmuir film balance. LPS Re monolayers exhibited purely viscous behaviour in the absence of calcium ions, while the same monolayers underwent a viscous-to-elastic transition upon compression in the presence of Ca^{2+}. Our results demonstrated for the first time that LPSs in bacterial outer membranes can form two-dimensional elastic networks in the presence of Ca^{2+}. Different from LPS Re monolayers, the LPS Ra monolayers showed a very similar rheological transition both in the presence and absence of Ca^{2+}, suggesting that longer saccharide chains can form 2D physical gels even in the absence of Ca^{2+}. By exposure of the monolayers to the antimicrobial peptide protamine, we could directly monitor the differences in resistance of bacterial membranes according to the presence of calcium.

Introduction

Lipopolysaccharides (LPSs, Chart 1) are a major component of the outermost membrane of Gram-negative bacteria. They do not only guarantee the structural integrity of bacteria but play key roles in many biological activities, such as sepsis.[1,2] Lipid A is the most fundamental building block with two phosphorylated *N*-acetylglucosamine units and six hydrocarbon chains. In addition they contain the R oligosaccharide unit (core), and a polydisperse polysaccharide chain (O-side chain). The core comprises (a) the inner core of four negatively charged saccharide units: two 2-keto-3-deoxyoctonoic acid (Kdo) units, and two phosphorylated heptose units, and (b) the outer core of five uncharged saccharides.[3,4]

Since the removal or mutation of LPSs is known to result in the death of Gram-negative bacteria, LPSs are supposed to play crucial roles in the structural integrity and resistance of bacteria against chemical attacks such as antimicrobial peptides. In fact, various antibacterial compounds have been designed as alternatives to chemical food preservatives and antibiotics in order to primarily target LPSs.[5] Protamine is a naturally occurring cationic peptide (isoelectric point at pH ≈ 10–12) in sperm cells of vertebrates, which is used in Japan as a food preservative. Many *in vivo* studies demonstrated that divalent cations (Ca^{2+}, Mg^{2+}) significantly increase the minimum inhibitory concentration (MIC) of protamine, *i.e.*, they protect bacteria against protamine. It has thus been suggested that electrostatic interactions are responsible for the interaction of the positively charged protamine molecules with the negatively charged LPS headgroups.[6–8]

There have been a number of studies on physical properties of lipopolysaccharide molecules and their aggregates, such as vibrational spectroscopic studies on molecular conformation,

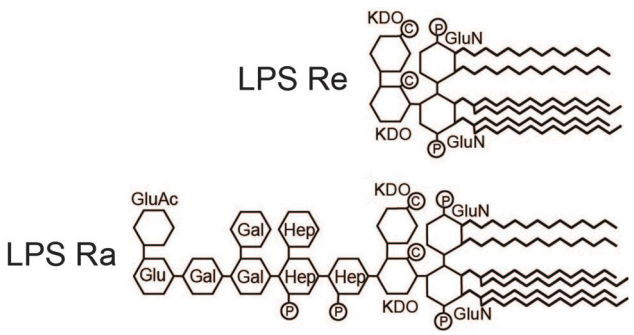

Chart 1 Chemical structures of lipopolysaccharides LPS Re (top) and LPS Ra (bottom).

[a] *Physical Chemistry of Biosystems, Institute of Physical Chemistry, University of Heidelberg, D69120 Heidelberg, Germany. E-mail: tanaka@uni-heidelberg.de*
[b] *Research Center Borstel, D23845 Borstel, Germany*
[c] *Institute for Integrated Cell-Material Sciences (WPI iCeMS), Kyoto University, 606-8501 Kyoto, Japan*

† Electronic supplementary information (ESI) available: Confirmation of linear response of LPS monolayer. See DOI: 10.1039/c5sm01002k

‡ Present address: Max Planck Institute of Colloids and Interfaces, D14476 Potsdam, Germany.

X-ray powder diffraction, and specular and off-specular neutron scattering.[9–16] In our previous accounts, we created a realistic model of bacterial outer membranes based on insoluble (Langmuir) monolayers of lipopolysaccharide from two bacterial strains: (1) *Salmonella enterica* sv. Minnesota R595 (LPS Re) that consists of lipid A and two Kdo units, and (2) *Salmonella enterica* sv. Minnesota R60 (LPS Ra) that only lacks the O-side chains with respect to wild-type LPSs.[9,17,18] The use of purified LPSs with monodisperse, short oligosaccharide headgroups enabled us to study their molecular organization under well-defined thermodynamic conditions, as well as to approximately describe the system as a set of distinct slabs with defined electron density, thickness, and interface roughness (slab model). Since it is known that lipid A is not sufficient for the bacterial growth, LPS Re can be considered as the minimal model of LPS. On the other hand, LPS Ra can be considered as the most realistic model LPS with defined saccharide head groups. We combined grazing incidence X-ray structural characterizations at the air/water interface and coarse-grained Monte Carlo simulations of LPS surfaces to determine the lateral ordering of hydrocarbon chains and electron density profiles perpendicular to the interface.[19] This unique combination enabled us to determine and interpret the structures of LPS Re and LPS Ra monolayers at Å resolution.[11,13–15] With LPS Re and LPS Ra we were further able to demonstrate that the condensation of divalent ions is crucial for bacteria to defend themselves against cationic antimicrobial peptides, which agrees well with the previous report suggesting a change in the water permeation in the presence of Ca^{2+}.[6–8,19–21] In the next step, to gain deeper insight into the electrostatics involved in this defense mechanism, the density profiles of monovalent and divalent cations normal to the LPS monolayers were determined by grazing-incidence X-ray fluorescence (GIXF), showing that divalent Ca^{2+} almost completely replaces monovalent K^+ from the interface when present.[22,23] On the other hand, despite of the fact that the LPS molecules play important roles in mechanically protecting bacteria against the membrane disruption caused by chemical/biochemical attacks, little is known about the impact of divalent cations on the mechanical properties of LPS surfaces.

Interfacial stress rheometry is a powerful technique to measure the dynamic viscous and elastic properties of molecular films on liquid surfaces.[24–26] Compared to the conventional rotating disk devices, interfacial stress rheometers (ISRs) achieve an approximately an order of magnitude higher sensitivity to surface stresses in the presence of bulk (subphase) stresses. The technique has been applied to monolayers of (i) synthetic surfactants, (ii) block copolymers and lipopolymers, and (iii) biological surfactants.[25,27–32] In our previous accounts, we studied by ISR the viscoelastic properties of synthetic glycolipid monolayers at the air/water interface under well-defined thermodynamic conditions. In particular, we studied the influence of the length and conformation of saccharide head groups on the monolayer mechanics.[33,34] Together with grazing-incidence X-ray diffraction the ISR measurements revealed that a transition from a predominantly viscous two-dimensional (2D) sol to an elastic 2D gel can be attributed to an in-plane cross-linking of the glycolipids *via* hydrogen bonding networks between the neutral saccharide head groups.[33,35]

In the present paper, we extend this strategy to study the mechanical properties of LPS monolayers. The dynamic viscous and elastic moduli of LPS monolayers were determined by using ISR in the presence and absence of divalent cations without disrupting the monolayers. Moreover, the impact of protamine on the mechanical properties of the LPS monolayers was investigated. This impact reflects the degree to which such antimicrobial peptides disturb the integrity of the monolayers. Details on the experimental results are discussed in the following sections.

Materials and methods

Materials, sample preparation

Deep rough mutant LPS (LPS Re) and LPS Ra (Chart 1) were extracted from *Salmonella enterica* (serovar Minnesota) strains R595 and R60, respectively. The purified samples were lyophilized according to the protocol described in previous reports.[9,17] MALDI-TOF mass spectrometry shows a sharp peak at 1797 Da, corresponding to the molecular weight of the lipid A portion with its hexa-acyl lipid anchors. Protamine extracted from herring sperm was purchased from Carl Roth GmbH (Germany) and dissolved in distilled, de-ionized water at a concentration of 0.1 g mL^{-1}.

The spreading solutions for the monolayer deposition were prepared by dissolving each LPS: LPS Re was dissolved into a mixture of chloroform/methanol (70/30 by volume) at a concentration of 2 mg mL^{-1}, while LPS Ra was dissolved into a mixture of petroleum ether/methanol/liquid phenol (9/3/2 by volume) at a concentration of 1 mg mL^{-1}. The use of different solvents for LPS Re and LPS Ra was necessary because of the significant difference in the hydrophilic/hydrophobic balance of the molecules and the resulting difference in their solubilities. After the deposition of the stock solution onto the aqueous subphase in a Langmuir trough (Nima Technology Ltd, UK) and the evaporation of the solvent (>15 min), the monolayer was compressed at a constant speed around 1 $Å^2$ per molecule per min. The area per molecule is proportional to the area of the air/water interface, which is controlled by the barriers of the Langmuir trough. The pre-factor depends on the amount of material deposited at the air/water interface prior to compression. The precise value of this pre-factor was determined by rescaling the area per molecule in the obtained isotherms (*i.e.*, the relation between area per molecule and surface pressure) to that in the well-known and published isotherms of LPS Re and LPS Ra on the same subphases.[20,23] The surface pressure π was determined *via* the force exerted to a hydrophilic Wilhelmy plate of known perimeter when partially dipped into the aqueous phase.[36] Water-insoluble (Langmuir-type) amphiphilic monolayers at air/water interfaces, such as the mutant LPS monolayers studied here, are well-controlled samples. The reproducibility of their preparation was confirmed by comparison of several independent isotherms for each condition. The reported rheological

properties of the monolayers were confirmed to be reproducible in control measurements on different monolayers prepared with the same protocol. To study the influence of Ca^{2+} ions, we used two types of buffer subphases (pH 7.4): (i) "Ca^{2+}-free" buffer that consists of 5 mM Hepes and 100 mM NaCl, and (ii) "Ca^{2+}-loaded" buffer that contains 5 mM Hepes, 100 mM NaCl, and 50 mM $CaCl_2$. The compositions of Ca^{2+}-free and Ca^{2+}-loaded sub-phases were chosen for direct comparability with earlier studies in which the protocol was established.[19,20,22,23] Note that the two sub-phases have different molarities and, as a result, different yet comparable Debye screening lengths. However, it is well known that the action of divalent cations goes far beyond the mere reduction of the screening length. In fact, our previous studies demonstrated that divalent Ca^{2+} displaces monovalent K^+ almost completely from the surface of LPS monolayers.[22,23] Note also that a comparison of different types of divalent cations is out of the scope of the present work.

Interfacial rheology

The viscoelastic properties of LPS monolayers at the air/water interface were studied by an interface stress rheometer (CIR-100, Camtel Inc. UK) coupled to the film balance. A small De Nouy ring made out of Pt wire (cross-sectional diameter of 0.28 mm, ring diameter of 13 mm) was partially immersed into the subphase. Here, a defined oscillatory shear stress can be applied to a film at the interface by driving the ring's rotation at controlled frequency ω and driving amplitude γ. The amplitude and phase shift of the ring's resulting rotation is then monitored, from which the dynamic surface modulus, $G^*(\omega) = G'(\omega) + iG''(\omega)$, is deduced as a complex function of ω. The real part of G^* (the shear storage modulus, G' [mN m^{-1}]) is a measure of the elastic properties, and the imaginary part (the shear loss modulus, G'' [mN m^{-1}]) represents the viscous properties.[37] G^* of the LPS monolayer can be represented by the damping (D) and elastic (K) response of the instrument in the presence (D, K) and absence of the monolayer (D_0, K_0), respectively:

$$G' = -\frac{C_s C_0}{RA}(K - K_0)$$

$$G'' = \frac{C_s C_0}{RA}(KD - K_0 D_f)$$

A is a geometric shape factor, C_s is the sensor constant, and C_0 and R are the galvanometric constant and the resistance of the instrument, respectively.[38] The immersion depth of the sensor ring was chosen at 0.14 mm from the point of first surface contact, where the sensitivity to the monolayer was found to be maximal. For each measurement the corresponding reference signal, *i.e.*, the aqueous subphase without a monolayer, was subtracted. The reference was measured with identical ring immersion depth. Statistical uncertainties in G' and G'' ($\delta G' = 0.21$ mN m^{-1}, $\delta G'' = 0.15$ mN m^{-1}) were estimated as the standard deviation of 10 data points in a time sweep experiment of a LPS Re monolayer compressed to a surface pressure of $\pi = 30$ mN m^{-1}. If not stated otherwise, the rheology experiments were carried out at 293 K, and the frequency and amplitude of the oscillation was set constant at $f = 5$ Hz and $\gamma = 1$ mrad throughout this study, after confirming that the system remains within the linear response regime (ESI†).

Results and discussion

Interfacial viscoelasticity of LPS Re monolayers

Fig. 1 represents the pressure–area isotherm (panel a) and the interfacial viscoelasticity (panel b) of LPS Re monolayers on Ca^{2+}-free subphase. As presented in Fig. 1a, the onset of the pressure increase upon compression was observed at $A \approx 215$ Å^2, and the plateau-like regime corresponding to the coexistence of fluid (liquid-expanded) and solid (liquid-condensed) phase appeared at $\pi \approx 25$–30 mN m^{-1}.[20] As presented in Fig. 1b, both viscous (G'') and elastic (G') modulus could not be detected up to the instrument resolution for molecular areas above $A \approx 160$ Å^2 ($\pi \approx 25$ mN m^{-1}). Even when the measurements were performed at larger strain amplitudes (3 and 4 mrad), both moduli stayed below the detection limit. Upon further compression of the monolayer, G'' showed a very small increase. However, with $G'' \approx 0.2$ mN m^{-1} the value still remained close to the detection limit, even at a condition close to the collapse of the monolayer, $A \approx 135$ Å^2. It should be noted that slightly negative values of G' are obtained under some measurement conditions, which is non-physical. However, this effect reflects a known

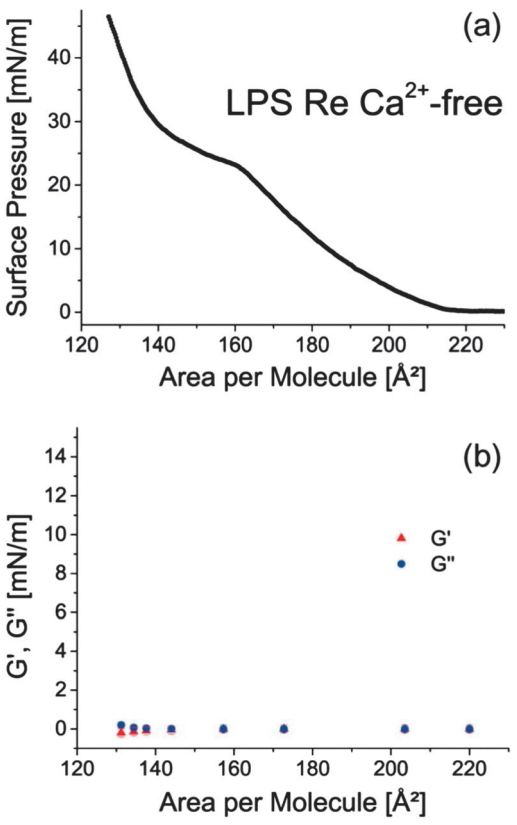

Fig. 1 (a) Pressure–area isotherm of LPS Re monolayer on Ca^{2+}-free subphase. (b) Viscous and elastic modulus of LPS Re monolayer on Ca^{2+}-free subphase. Error bars are comparable to the symbol size and therefore not visible.

measurement artifact of the instrument (see ESI†), and its magnitude is comparable with the measurement precision, much weaker than the discussed trends. In summary, the obtained results imply that the LPS Re monolayer on Ca^{2+}-free subphase remains almost like a Newtonian fluid, which is predominantly viscous even at high surface pressures close to the film collapse. The Newtonian behavior is further confirmed in the ESI† (Fig. S1), where a flow curve (G'' *vs.* frequency) is presented for LPS Re on Ca^{2+}-free subphase at high compression ($A \approx 133$ Å^2).

Fig. 2 represents the pressure–area isotherm (panel a) and the interfacial viscoelasticity (panel b) of LPS Re monolayers on Ca^{2+}-loaded subphase. In contrast to the results on Ca^{2+}-free subphase (Fig. 1a), the onset of pressure increase appeared at much lower area per molecule $A \approx 185$ Å^2. Furthermore, the coexistence of liquid-expanded and liquid-condensed phase was found at much lower surface pressure, $\pi \approx 15$–20 mN m^{-1}, suggesting that Ca^{2+} substantially reduces the repulsion between LPS Re molecules.[20]

Similar to the results on Ca^{2+}-free subphase (Fig. 1b), the viscous and elastic moduli of LPS Re monolayers on Ca^{2+}-loaded subphase could not be detected for molecular areas above $A \approx 150$ Å^2. In contrast to the results on Ca^{2+}-free subphase, the viscous modulus showed a prominent increase, up to $G'' \approx 3.7$ mN m^{-1} at $A \approx 127$ Å^2 ($\pi \approx 33$ mN m^{-1}). This seems to agree well with the values for synthetic phospholipids and glycolipids in liquid condensed phase, suggesting that the increase in G'' is mainly caused by the condensation of hydrocarbon chains.[33,34] In fact, the lateral chain compressibility of these monolayers at $\pi \approx 25$–40 mN m^{-1} is in the order of $\chi = -1/A(\partial A/\partial \pi) \approx 0.01$ mN^{-1} m, showing very good agreement with those reported for phospholipid monolayers.[19]

Upon compression from $A = 155$ Å^2 to $A = 127$ Å^2 ($\pi = 33$ mN m^{-1}) the monolayer also shows a significant increase of the elastic modulus to $G' = 14$ mN m^{-1}, which is more than 3 times larger than the viscous modulus. The cross-over point of G' and G'' observed at $A \approx 132$ Å^2 demarks the rheological transition from a predominantly viscous two-dimensional fluid ($G'' > G'$) to an elastic two-dimensional physical gel ($G' > G''$).

We previously measured the interfacial rheology of uncharged synthetic glycolipid monolayers and investigated how the length and conformation of saccharide head groups would influence the viscoelastic properties of monolayers.[33,34] Among four different glycolipids, we found that only lipids with tri-lactose head groups underwent such a rheological transition upon compression. This finding can be explained in terms of the formation of hydrogen bonds between oligosaccharide head groups, which was supported by the small- and wide-angle X-ray scattering as well as by the grazing-incidence X-ray diffraction.[35,39] The hydrogen bonding effect on the interface rheology of glycolipids was further investigated by using D_2O subphase, which causes slightly stronger hydrogen bonding characteristics.[34,40,41] The results obtained in the present study are the first report on the formation of two-dimensional gels in biomimetic monolayers caused by cross-linking of charged saccharide head groups *via* divalent cations.

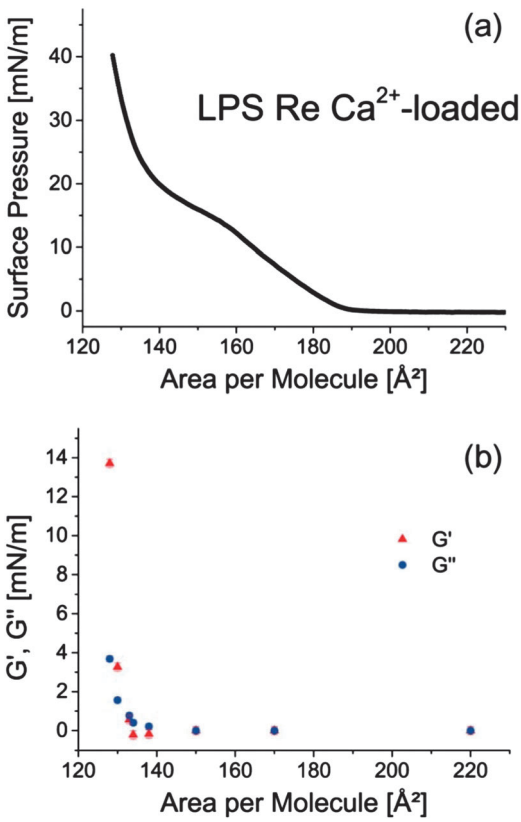

Fig. 2 (a) Pressure–area isotherm of LPS Re monolayer on Ca^{2+}-loaded subphase. (b) Viscous and elastic modulus of LPS Re monolayer on Ca^{2+}-loaded subphase. Error bars are comparable to the symbol size and therefore not visible.

Interfacial viscoelasticity of LPS Ra monolayers

Fig. 3 represents the pressure–area isotherm (panel a) and the interfacial viscoelasticity (panel b) of LPS Ra monolayers on Ca^{2+}-free subphase. The absence of a plateau-like regime suggests that the hydrocarbon chains remain disordered (fluid). Indeed, grazing-incidence X-ray diffraction confirmed that no Bragg peak could be detected at all lateral pressures.[19] The onset of pressure increase upon compression appears at a much larger area per molecule ($A \approx 320$ Å^2) than the corresponding value for the LPS Re monolayer on the same subphase ($A \approx 215$ Å^2), which can be explained by the bulkier head group of LPS Ra.

As presented in Fig. 3b, the viscous modulus of the LPS Ra monolayer on Ca^{2+}-free subphase showed a clear increase upon the compression to $A < 180$ Å^2. The viscous modulus at $A = 172$ Å^2 ($\pi = 41$ mN m^{-1}) is $G'' = 1.7$ mN m^{-1}, which is about an order of magnitude larger than the corresponding value ($G'' = 0.2$ mN m^{-1}) of LPS Re monolayers on the same subphase at a much higher surface pressure ($\pi = 33$ mN m^{-1}). In contrast to LPS Re monolayers that showed no detectable elastic response in the absence of Ca^{2+}, the LPS Ra monolayer underwent a rheological transition to predominantly elastic behaviour at $A \approx 178$ Å^2. The value of elastic modulus at $A = 172$ Å^2 ($G' = 6.9$ mN m^{-1}) suggests that the bulkier LPS Ra head groups can

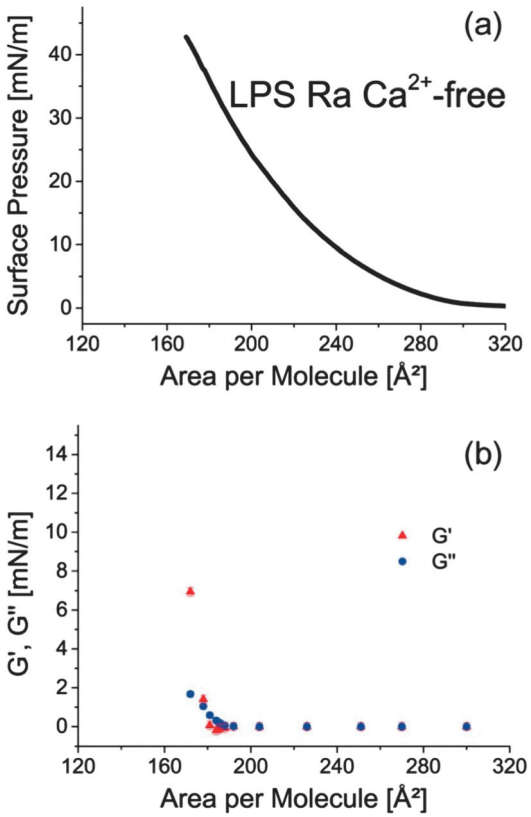

Fig. 3 (a) Pressure–area isotherm of LPS Ra monolayer on Ca^{2+}-free subphase. (b) Viscous and elastic modulus of LPS Ra monolayers on Ca^{2+}-free subphase. Error bars are comparable to the symbol size and therefore not visible.

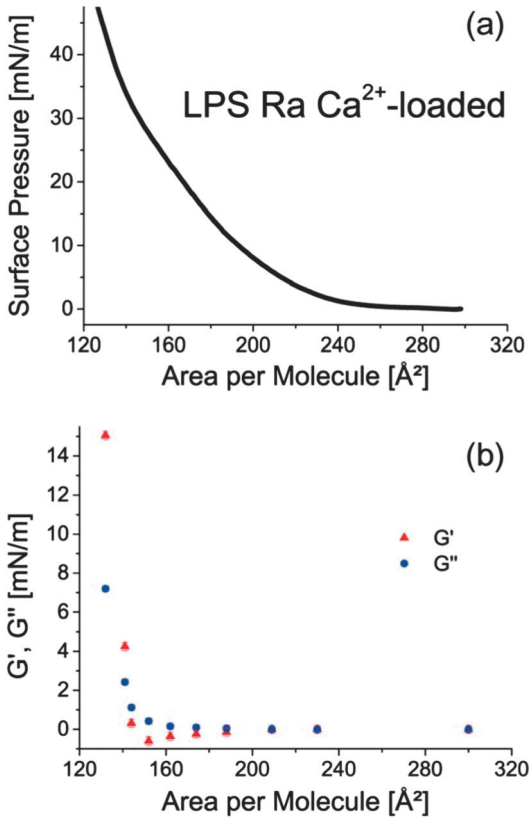

Fig. 4 (a) Pressure–area isotherm of LPS Ra monolayer on Ca^{2+}-loaded subphase. (b) Viscous and elastic modulus of LPS Ra monolayers on Ca^{2+}-loaded subphase. Error bars are comparable to the symbol size and therefore not visible.

form two-dimensional gels even in the absence of Ca^{2+} at a high packing density. It should be noted that measurements of the viscous and elastic modulus at $A < 170$ Å^2 were practically impossible, as the LPS Ra monolayers were very close to the collapse condition.

The pressure–area isotherm and the interfacial viscoelasticity of LPS Ra monolayers on Ca^{2+}-loaded subphase are presented in Fig. 4a and b, respectively. Different from LPS Re, the isotherm of LPS Ra showed no plateau-like regime even in the presence of Ca^{2+} due to the lack of a transition to periodic chain ordering. In comparison to the isotherm of the LPS Ra on Ca^{2+}-free subphase (Fig. 3a), the onset of the pressure increase upon compression appears at a much smaller area per molecule, $A \approx 260$ Å^2. Moreover, the lateral chain compressibility χ of the LPS Ra monolayer on Ca^{2+}-loaded subphase is always smaller than that on Ca^{2+}-free subphase throughout the experiments, suggesting that the LPS Ra molecules are more laterally compacted in the presence of Ca^{2+}. The viscous modulus of the LPS Ra monolayer on Ca^{2+}-loaded subphase showed a monotonic increase upon compression to smaller areas per molecule (Fig. 4b), resulting in $G'' = 7.2$ mN m^{-1} at $A = 132$ Å^2 ($\pi = 41$ mN m^{-1}). This value is in the same order of magnitude to the viscous modulus of the LPS Ra monolayer on Ca^{2+}-free subphase at a comparable surface pressure, $\pi = 41$ mN m^{-1}. Furthermore, the LPS Ra monolayer underwent a clear rheological transition at $A \approx 145$ Å^2. The area per molecule at which the cross-over of G' and G'' was observed was smaller than that in the absence of Ca^{2+} at $A \approx 178$ Å^2, which can be attributed to the compaction of LPS Ra monolayers in the presence of Ca^{2+}. At $A < 130$ Å^2, the LPS Ra monolayers became so unstable that the measurements of dynamic modulus were not possible. The fact that the LPS Ra monolayers undergo rheological transitions from a viscous 2D sol to an elastic gel both in the presence and absence of Ca^{2+} can be interpreted in terms of the hydrogen bond formation between the longer and bulkier saccharide head groups. An earlier study of Naumann *et al.* reported that monolayers of phosphatidylethanolamines modified with polyethyleneglycol chains underwent a viscous-to-elastic rheological transition near the end point of phase coexistence.[27] In contrast, we found that the formation of 2D gels in LPS Ra monolayers is not correlated to the ordering of hydrocarbon chains.

Impact of protamine on interfacial viscoelasticity

The viscous and elastic moduli of an LPS Re monolayer upon injection of protamine into the subphase are plotted as a function of time in Fig. 5. In the absence of Ca^{2+} (Fig. 5a), the monolayer was compressed up to $\pi = 30$ mN m^{-1}. After the equilibration, protamine was injected into the subphase to reach a final concentration of 1 mg mL^{-1} (comparable to MIC), while keeping the monolayer area constant. After an abrupt jump in

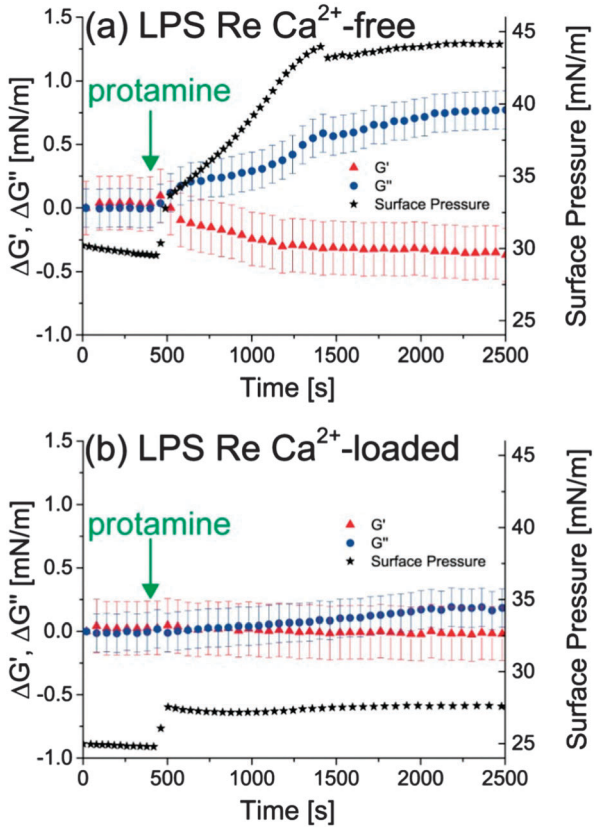

Fig. 5 (a) Rheological response of LPS Re without Ca^{2+}: surface pressure rises from π = 30 to 45 mN m^{-1}. (b) Rheological response of LPS Re with Ca^{2+}: surface pressure rises from π = 24 to 27 mN m^{-1}.

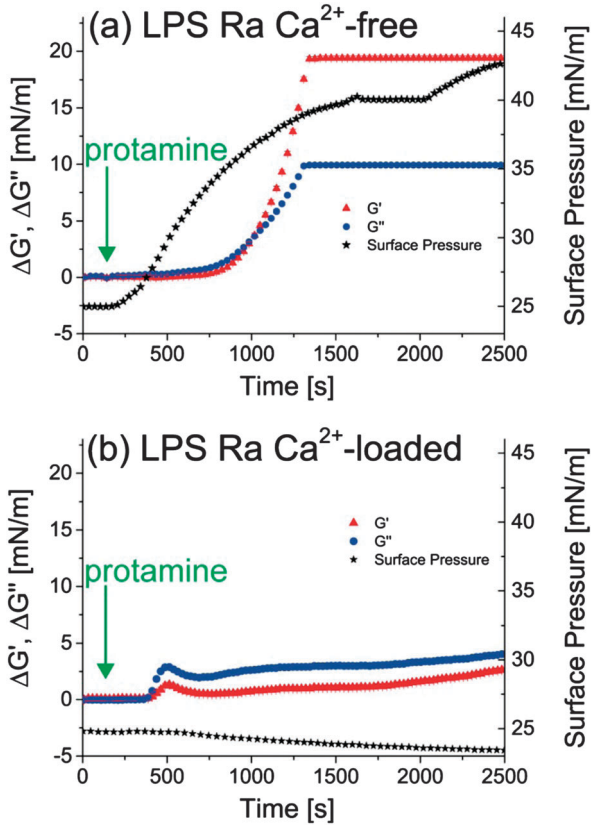

Fig. 6 (a) Rheological response of LPS Ra without Ca^{2+}: surface pressure rises from π = 25 to 38 mN m^{-1}. (b) Rheological response of LPS Ra with Ca^{2+}: surface pressure falls from π = 25 to 24 mN m^{-1}. Error bars are comparable to the symbol size and therefore not visible.

π upon the injection ($\Delta\pi \approx 3$ mN m^{-1}), the surface pressure showed a rapid increase up to $\pi \approx 45$ mN m^{-1} within 30 min. The pronounced increase in the surface pressure ($\Delta\pi \approx 15$ mN m^{-1}) observed here is consistent with our previous report, suggesting that the protamine molecules go into the hydrophobic core region and disrupt the monolayer structure.[20] According to the increase in the surface pressure, the viscous modulus also increased from undetectably low values to $G'' \approx 0.7$ mN m^{-1} after 30 min. On Ca^{2+}-loaded subphase, a completely different mechanical response was observed (Fig. 5b). Here, the monolayer was compressed to $\pi \approx 25$ mN m^{-1} prior to the protamine injection. After an abrupt jump upon the injection ($\Delta\pi \approx 3$ mN m^{-1}), the surface pressure remained constant over 30 min. Changes in the viscous modulus were at the detection limit ($\Delta G'' < 0.2$ mN m^{-1}). Changes in the elastic modulus were not detectable. This finding is fully consistent with our previous X-ray scattering study, demonstrating that the structures of the LPS Re monolayers perpendicular to the air/water interface were not influenced by protamine in the presence of Ca^{2+}.[19]

In the case of LPS Ra monolayers, the viscoelasticity measurements were carried out after the compression of monolayers to $\pi \approx 25$ mN m^{-1}. It should be noted that measurements at higher surface pressures were not practically possible, because the monolayers became mechanically unstable. As presented in Fig. 6a, the injection of protamine led to a increase in the surface pressure in the absence of Ca^{2+}, resulting in π = 38 mN m^{-1} after 20 min. Different from the LPS Re monolayers (Fig. 5a), both viscous and elastic modulus showed substantial increase after a delay of $t \approx 10$ min. After the onset of the increase in viscoelasticity, both viscous and elastic modulus increased significantly and underwent a rheological transition into a predominantly elastic 2D gel. Shortly after the cross-over, the elastic modulus reached to the upper detection limit. In contrast, in the presence of Ca^{2+} (Fig. 6b), the surface pressure remained almost identical. Similar to the system on Ca^{2+}-free subphase, the viscous and elastic modulus changed after a delay of $t \approx 3$ min. Here, changes in elastic ($\Delta G'$ = 1 mN m^{-1}) and viscous modulus ($\Delta G''$ = 3 mN m^{-1}) were much smaller than the changes observed on Ca^{2+}-free subphase, which suggests that LPS Ra monolayers stayed mechanically intact in the presence of Ca^{2+}.

Conclusions

In this paper, the interfacial viscoelastic properties of monolayers of bacterial lipopolysaccharides (LPS Re and LPS Ra) have been determined by using an interfacial rheometer coupled to a Langmuir film balance. In the absence of Ca^{2+} the monolayer of the minimum lipopolysaccharide model (LPS Re) behaved like a two-dimensional (2D) Newtonian fluid, while the same

monolayer underwent a clear viscous-to-elastic transition in the presence of Ca^{2+}. The obtained results demonstrated for the first time that LPSs in bacterial outer membranes can form physically cross-linked, 2D elastic gels in the presence of Ca^{2+}. Different from LPS Re monolayers, the more complex LPS Ra monolayers showed a very similar rheological transition both in the presence and absence of Ca^{2+}, suggesting that longer and bulkier saccharide chains can form hydrogen bonding networks and thus 2D physical gels even in the absence of Ca^{2+}. When protamine was injected at a concentration close to the MIC, the monolayers stayed intact only in the presence of Ca^{2+}. This experimental finding is consistent with our previous structural characterization, demonstrating that the cross-linking of Kdo cores with Ca^{2+} is essential for the resistance of bacterial outer membranes against the attack by cationic antibacterial peptides. The obtained results provide with the first mechanistic evidence that physically cross-linked, 2D highly viscoelastic films of LPSs "mechanically" protect gram negative bacteria against the intrusion of cationic peptides.

Acknowledgements

This work was supported by the German Science Foundation (Ta 259/5, Ta 259/12), the Canadian Centre of Excellence "Advanced Food and Materials Network", EUFP7 BIBAFOODS, and JSPS KAKENHI (26247070, 26103521). M.T. and E.S. thank J. M. Poeschl, D. A. Pink, and T. Beveridge for stimulating discussion. E.S. acknowledges support from a Marie Curie Intra-European Fellowship within the European Commission seventh Framework Program. M.T. is a member of the German Cluster of Excellence "Cell Networks". The iCeMS is supported by World Premier International Research Center Initiative (WPI), MEXT, Japan.

Notes and references

1 P. S. Tobias, J. C. Mathison and R. J. Ulevitch, *J. Biol. Chem.*, 1988, **263**, 13479–13481.
2 J. M. B. Pöschl, C. Leray, P. Ruef, J. P. Cazenave and O. Linderkamp, *Crit. Care Med.*, 2003, **31**, 924–928.
3 D. L. Nelson and M. M. Cox, *Lehninger Principles of Biochemistry*, W. H. Freeman, New York, 2008.
4 K. Brandenburg, J. Andrä, M. Müller, M. H. J. Koch and P. Garidel, *Carbohydr. Res.*, 2003, **338**, 2477–2489.
5 R. E. W. Hancock and D. S. Chapple, *Antimicrob. Agents Chemother.*, 1999, **43**, 1317–1323.
6 T. D. Brock, *Can. J. Microbiol.*, 1958, **4**, 65–71.
7 L. T. Hansen, J. W. Austin and T. A. Gill, *Int. J. Food Microbiol.*, 2001, **66**, 149–161.
8 N. M. Islam, T. Itakura and T. Motohiro, *Bull. Jpn. Soc. Sci. Fish.*, 1984, **50**, 1705–1708.
9 K. Brandenburg and U. Seydel, *Biochim. Biophys. Acta*, 1984, **775**, 225.
10 K. Brandenburg, *Biophys. J.*, 1993, **64**, 1215–1231.
11 K. Brandenburg, M. H. J. Koch and U. Seydel, *J. Struct. Biol.*, 1992, **108**, 93–106.
12 D. Naumann, C. Schultz, A. Sabisch, M. Kastowsky and H. Labischinski, *J. Mol. Struct.*, 1989, **214**, 213–246.
13 M. Kastowsky, T. Gutberlet and H. Bradaczek, *Eur. J. Biochem.*, 1993, **217**, 771–779.
14 U. Seydel, M. H. J. Koch and K. Brandenburg, *J. Struct. Biol.*, 1993, **110**, 232–243.
15 T. Abraham, S. R. Schooling, M.-P. Nieh, N. Kučerka, T. J. Beveridge and J. Katsaras, *J. Phys. Chem. B*, 2007, **111**, 2477–2483.
16 E. Schneck, R. G. Oliveira, F. Rehfeldt, B. Demé, K. Brandenburg, U. Seydel and M. Tanaka, *Phys. Rev. E: Stat., Nonlinear, Soft Matter Phys.*, 2009, **80**, 041929.
17 C. Galanos, O. Lüderitz and O. Westphal, *Eur. J. Biochem.*, 1969, **9**, 254.
18 B. Jiao, M. Freudenberg and C. Galanos, *Eur. J. Biochem.*, 1989, **180**, 515–518.
19 R. G. Oliveira, E. Schneck, B. E. Quinn, O. V. Konovalov, K. Brandenburg, U. Seydel, T. Gill, C. B. Hanna, D. A. Pink and M. Tanaka, *CR Chim.*, 2009, **12**, 209–217.
20 R. G. Oliveira, E. Schneck, B. E. Quinn, O. V. Konovalov, K. Brandenburg, T. Gutsmann, T. Gill, C. B. Hanna, D. A. Pink and M. Tanaka, *Phys. Rev. E: Stat., Nonlinear, Soft Matter Phys.*, 2010, **81**, 041901.
21 N. Kučerka, E. Papp-Szabo, M.-P. Nieh, T. A. Harroun, S. R. Schooling, J. Pencer, E. A. Nicholson, T. J. Beveridge and J. Katsaras, *J. Phys. Chem. B*, 2008, **112**, 8057–8062.
22 E. Schneck, T. Schubert, O. V. Konovalov, B. E. Quinn, T. Gutsmann, K. Brandenburg, R. G. Oliveira, D. A. Pink and M. Tanaka, *Proc. Natl. Acad. Sci. U. S. A.*, 2010, **107**, 9147–9151.
23 W. Abuillan, E. Schneck, A. Körner, K. Brandenburg, T. Gutsmann, T. Gill, A. Vorobiev, O. Konovalov and M. Tanaka, *Phys. Rev. E: Stat., Nonlinear, Soft Matter Phys.*, 2013, **88**, 012705.
24 R. Miller, L. Liggieri and V. V. Krotov, *Interfacial rheology*, Brill, Leiden, Boston, 2009.
25 C. F. Brooks, G. G. Fuller, C. W. Franck and C. R. Robertson, *Langmuir*, 1999, **15**, 2450–2459.
26 P. Cicuta, E. J. Stancik and G. G. Fuller, *Phys. Rev. Lett.*, 2003, **90**, 236101.
27 C. A. Naumann, C. F. Brooks, G. G. Fuller, T. Lehmann, J. Rühe, W. Knoll, P. Kuhn, O. Nuyken and C. W. Frank, *Langmuir*, 2001, **17**, 2801–2806.
28 C. Luap and W. A. Goedel, *Macromolecules*, 2001, **34**, 1343–1351.
29 C. Monteux, R. Mangeret, G. Laibe, E. Freyssingeas, V. Bergeron and G. Fuller, *Macromolecules*, 2006, **39**, 3408–3414.
30 J. W. Anseth, A. J. Goffin, G. G. Fuller, A. J. Ghio, P. N. Kao and D. Upadhyay, *Am. J. Respir. Cell Mol. Biol.*, 2005, **33**, 161–168.
31 S. Y. Nishimura, G. M. Magana, H. A. Ketelson and G. G. Fuller, *Langmuir*, 2008, **24**, 11728–11733.
32 C. Wu, J. Y. Lim, G. G. Fuller and L. Cegelski, *Biophys. J.*, 2012, **103**, 464–471.
33 M. F. Schneider, K. Lim, G. G. Fuller and M. Tanaka, *Phys. Chem. Chem. Phys.*, 2002, **4**, 1949–1952.
34 M. Tanaka, S. Schiefer, C. Gege, R. R. Schmidt and G. G. Fuller, *J. Phys. Chem. B*, 2004, **108**, 3211–3214.

35 M. Tanaka, M. F. Schneider and G. Brezesinski, *ChemPhysChem*, 2003, **4**, 1316–1322.
36 K. Holmberg, D. O. Shah and M. J. Schwuger, *Handbook of applied surface and colloid chemistry*, Wiley, Chichester, England, New York, 2002.
37 D. A. Edwards, H. Brenner and D. T. Wasan, *Interfacial Transport Processes and Rheology*, Butterworth-Heinemann, Burlington, 1991.
38 M. Sheriff and B. Warburton, ed. K. Walters, J. F. Hutton and J. R. A. Pearson, *Theoretical Rheology*, Applied Science Publishers, London, 1975.
39 M. F. Schneider, R. Zantl, C. Gege, R. R. Schmidt, M. Rappolt and M. Tanaka, *Biophys. J.*, 2003, **84**, 306–313.
40 J. C. Dore, *J. Mol. Struct.*, 1991, **250**, 193–211.
41 M. F. Chaplin, *Biophys. Chem.*, 2000, **83**, 211–221.

